BJR

https://doi.org/10.1259/bjr.20160778

Received: 30 September 2016 | Revised: 14 June 2017 | Accepted: 7 August 2017

Cite this article as:
Aissa J, Boos J, Sawicki LM, Heinzler N, Krzymyk K, Sedlmair M, et al. Iterative metal artefact reduction (MAR) in postsurgical chest CT: comparison of three iMAR-algorithms. *Br J Radiol* 2017; **90**: 20160778.

FULL PAPER

Iterative metal artefact reduction (MAR) in postsurgical chest CT: comparison of three iMAR-algorithms

[1]JOEL AISSA, MD, [1]JOHANNES BOOS, MD, [1]LINO MORRIS SAWICKI, MD, [1]NIKLAS HEINZLER, MD, [2]KARL KRZYMYK, MR, [3]MARTIN SEDLMAIR, PhD, [1]PATRIC KRÖPIL, MD, [1]GERALD ANTOCH, MD and [1]CHRISTOPH THOMAS, MD

Department of Diagnostic and Interventional Radiology, University Dusseldorf, Medical Faculty, Dusseldorf, Germany
Department of Computed Tomography, Siemens Healthineers GmH, Cologne, Germany
Department of Computed Tomography, Siemens Healthineers GmH, Forchheim, Germany

Address correspondence to: Dr med Joel Aissa
E-mail: *Joel.Aissa@med.uni-duesseldorf.de*

Objectives: The purpose of this study was to evaluate the impact of three novel iterative metal artefact (iMAR) algorithms on image quality and artefact degree in chest CT of patients with a variety of thoracic metallic implants.
Methods: 27 postsurgical patients with thoracic implants who underwent clinical chest CT between March and May 2015 in clinical routine were retrospectively included. Images were retrospectively reconstructed with standard weighted filtered back projection (WFBP) and with three iMAR algorithms (iMAR-Algo1 = Cardiac algorithm, iMAR-Algo2 = Pacemaker algorithm and iMAR-Algo3 = ThoracicCoils algorithm). The subjective and objective image quality was assessed.
Results: Averaged over all artefacts, artefact degree was significantly lower for the iMAR-Algo1 (58.9 ± 48.5 HU), iMAR-Algo2 (52.7 ± 46.8 HU) and the iMAR-Algo3 (51.9 ± 46.1 HU) compared with WFBP (91.6 ± 81.6 HU, $p < 0.01$ for all). All iMAR reconstructed images showed significantly lower artefacts ($p < 0.01$) compared with the WFPB while there was no significant difference between the iMAR algorithms, respectively. iMAR-Algo2 and iMAR-Algo3 reconstructions decreased mild and moderate artefacts compared with WFBP and iMAR-Algo1 ($p < 0.01$).
Conclusion: All three iMAR algorithms led to a significant reduction of metal artefacts and increase in overall image quality compared with WFBP in chest CT of patients with metallic implants in subjective and objective analysis. The iMARAlgo2 and iMARAlgo3 were best for mild artefacts. IMARAlgo1 was superior for severe artefacts.
Advances in knowledge: Iterative MAR led to significant artefact reduction and increase image-quality compared with WFBP in CT after implementation of thoracic devices. Adjusting iMAR-algorithms to patients' metallic implants can help to improve image quality in CT.

INTRODUCTION

Thoracic CT is routinely performed for diagnosis of thoracic pathologies. This includes assessment of lung pathologies, vascular structures and mediastinal or cardiac pathologies as well as spine and trauma imaging. Furthermore, CT reflects the method of choice in the detection of postoperative complications and is also frequently used in the follow up of patients after thoracic surgery.[1] Complications from thoracic surgery commonly assessed with chest CT include infections, sternal displacements, osteomyelitis, thoracic hemorrhage or pneumothorax.[1,2]

Sternotomy is one of the most frequently used access strategies for various thoracic surgeries such as coronary artery bypass surgery, cardiac valve replacement and open-heart surgery.[3] These surgeries often lead to intrathoracic implantation of metallic devices such as pacemakers, valve replacements or left ventricular assistant devices.[4,5] Furthermore, sternal wire closure is commonly performed to close up the surgical access route.

Metallic implants from thoracic surgery can lead to fine streak artefacts as well as broader dark or bright band artefacts in CT.[4] These artefacts can hamper image quality in CT and limit diagnostic capability. Severe artefacts can mask acute complications like bleeding or abscesses adjacent to the metallic hardware.

To reduce artefacts from metal implants in CT, different approaches have been introduced.[6–8] With the increase in

Figure 1. Chest CT after left ventricular assist device implementation reconstructed with weighted filtered back projection in soft tissue window and bone window. These pictures demonstrate severe streak artefacts produced by chest implants. Especially, retroperitoneal structures like thoracic aorta or lung parenchyma are masked by streak artefacts (arrow).

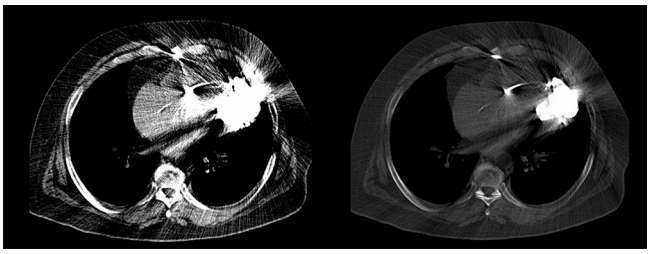

available computational power, novel iterative MAR (iMAR) techniques have become available recently (Figure 1). Research so far has mainly focused on iMAR in patients with large orthopedic implants,[9] dental hardware or vertebral implants.[10,11] To our knowledge, the value of iMAR in the setting of thoracic metallic implants has not been investigated yet. However, artefacts from metallic implants are a continuing challenge in patients following thoracic surgery, and efficient algorithms to improve image quality in these patients are desirable.

Therefore, the aim of this study was to investigate the impact of three novel iMAR algorithms on image quality and artefact degree in chest CT of patients with thoracic metallic implants.

METHODS AND MATERIALS

This retrospective study was approved by the local ethics committee.

Patients

27 postsurgical patients (22 males, 5 females, mean age: 68.1 ± 11.1 years, range: 44–82 years) who underwent chest CT between March and May 2015 in clinical routine were retrospectively included in the analysis. Metal objects (n = 38) included sternal steel wiring (n = 25), left ventricular assist devices (n = 3), port systems which all were located within the chest wall (n = 3), cardiac pacemakers (n = 3) and extracorporeal devices (n = 4). We found in 13 of 27 patients two different types of metal objects.

Image acquisition

Examinations were performed on a 64-section slice CT scanner with sliding gantry capability (n = 13; Siemens Somatom Definition Sliding Gantry, Siemens Healthcare GmbH, Erlangen, Germany) and a 128-section dual source CT scanner (n = 14; Somatom Definition Flash, Siemens Healthcare GmbH). Scans were performed with automated tube current modulation (CareDose4D, Siemens Healthcare GmbH) with a mean tube current of 163 ± 61.8 mAs and automatic tube voltage selection (100 kV, n = 21; 120 kV, n = 6). Rotation time was 0.5 s and collimation was 0.6 mm in all scans. All scans were performed in supine position and on inspiration.

All scans were performed after body-weight-adapted intravenous injection of iodine-containing contrast media (Imeron 400, Bracco Imaging Deutschland GmbH, Konstanz, Germany and Accupaque 300 mg, GE Healthcare Buchler GmbH & Co, München, Germany) and bolus triggering.

Image processing

All images for the study were retrospectively reconstructed on a workstation using prototype software (ReconCT 13.8.2.0, Siemens Healthcare GmbH, Erlangen, Germany). Reconstructions were performed with standard weighted filtered back projection (WFBP; Siemens Healthcare GmbH) and additionally with three iMAR algorithms (iMAR 2D, iMAR-Algo1 = Cardiac algorithm, iMAR-Algo2 = Pacemaker algorithm and iMAR-Algo3 = ThoracicCoils algorithm, Siemens Healthcare GmbH, respectively). The reconstructed WFBP images do refer to our clinical-filtered back projection images without other MAR options. WFBP images as well as post-processed images with the iMAR algorithms were reconstructed in axial orientation and a slice thickness of 5 mm using a soft tissue kernel (B30f). For subjective and objective image analysis in this study, 5 mm slices are sufficient, therefore we consequently renounced on thinner reconstructions. Reconstructed images were archived in the picture archiving and communication system (PACS, Sectra Medical Systems GmbH, Linköping, Sweden). WFBP reconstructions served as reference standard in this study.

Subjective image analysis

Subjective image quality and image artefacts were evaluated by two independent readers (BLINDED, consultant grade radiologist and BLINDED with 5 and 4 years of experience in reading chest CT).

For overall image quality, one single overall score was given with regard to metallic hardware, osseous structures, soft tissue and lung parenchyma. Overall image quality was rated on a five-point scale according to previous studies (1: severe artefacts, non-diagnostic; 2: poor image quality, partly non-diagnostic; 3: moderate image quality, limited diagnostic confidence; 4: good image quality, sufficient for diagnosis; 5: excellent image quality, no artefacts).[12] Based on the overall image quality, implants were divided into devices producing severe artefacts (image quality 1–2) and implants generating moderate-to-no artefacts ("mild artefacts") (image quality 3–5).

Furthermore, overall artefact degree was rated separately for near field (<3 cm from the metal) and far field (≥3 cm from the metal) on a five-point scale according to previous studies[13] (1: severe artefacts; 2: strong artefacts; 3: moderate artefacts; 4: mild artefacts; 5: no artefact).

Artefacts were rated in a random order on a PACS workstation (Sectra Medical Systems GmbH, Linköping, Sweden). Adjustment of the window was to the discretion of the readers. Readers were blinded to patient data and image reconstruction parameters.

Objective image analysis

Quantitative analysis of MAR was performed according to previous studies.[4,14] Oval region of interest (diameter: 1–4 cm)

measurements were performed in three different locations adjacent to each metallic implant and standard deviations (SD; in Hounsfield Units, HU) were recorded. Regions of interest were measured on slices with the strongest artefact level as judged visually. Mean standard deviation of the three measurements was calculated to account for objective artefact degree; therefore, higher values of SD reflect higher artefact load. Measurements were performed by one reader (BLINDED) on a PACS workstation (Sectra Medical Systems GmbH, Linköping, Sweden).

Statistical analysis

All data are given in mean ± standard deviation. Data analysis was performed using IBM SPSS Statistics 22™ for Windows (SPSS, Chicago, IL). Statistical significance was set to $p < 0.05$. A Kolmogorov test was performed to test for normality. Analysis of variance was performed for normally distributed variables. A Wilcoxon test was used as non-parametric test. Bonferroni method was used to correct for multiple testing. Kappa-value was calculated to evaluate the inter-observer agreement. Interobserver agreement was defined as excellent ($\kappa > 0.81$), good ($\kappa = 0.61–0.80$), moderate ($\kappa = 0.41–0.60$), fair ($\kappa = 0.21–0.40$) and poor ($k \leq 0.20$).[15]

RESULTS

Subjective image analysis

Overall artifacts

Mild metallic artefacts were found in 27/38 (71%) of thoracic metallic implants. These were caused by sternal steel wiring ($n = 25$), port systems ($n = 1$) and overlying devices ($n = 1$). Severe metallic artefacts were found in 11/38 (29%) of implants, caused by LVADs ($n = 3$), overlying devices (ECG cables) ($n = 3$), port systems/pacemakers ($n = 4$) and an aortic valve prosthesis ($n = 1$).

Mild artefacts

Regarding mild-to-moderate artefacts, these were strongest for WFBP (near field: 3.6 ± 0.5, far field 4.5 ± 0.6) and iMAR-Algo1 algorithm (near field: 3.8 ± 0.5, far field 4.7 ± 0.5). We found significantly lower mild-to-moderate artefacts for the iMAR-Algo2 and iMAR-Algo3 reconstructions (near field: 4.5 ± 0.5, far field 4.9 ± 0.2 and near field: 4.5 ± 0.5, far field 4.9 ± 0.3, respectively) compared with WFBP and iMARAlgo1 ($p < 0.01$ for both; Table 1).

Severe artefacts

Concerning severe artefacts, we found strongest artefacts for WFBP reconstructed images (near field: 1.7 ± 0.4, far field 2.5 ± 0.6). All iMAR reconstructed images (iMAR-Algo1: near field: 3.8 ± 0.4, far field 4.2 ± 0.5; iMAR-Algo2: near field: 3.3 ± 0.5, far field 3.5 ± 0.5; iMAR-Algo3: near field: 3.3 ± 0.5, far field 3.5 ± 0.5) showed significantly lower artefacts ($p < 0.01$) compared with the standard reconstructions while there was no significant difference between the iMAR algorithms, respectively (Table 1). We found no new induced MAR artefacts due to any of the iMAR algorithms.

Overall image quality

All reconstructions showed diagnostic image quality. Mean overall score for WFBP as standard reconstruction method was 3.1 ± 1.3. Mean overall scores for the iMAR algorithms were 3.8 ± 0.1 for iMAR-Algo1, 4.3 ± 0.8 for iMAR-Algo2 and 4.2 ± 0.7 for iMAR-Algo3. All iMAR algorithms showed a significantly better overall image quality compared with WFBP reconstructions ($p < 0.01$, respectively). Overall image quality did not differ significantly between CT images reconstructed with WFBP and the iMARAlgo1. Interobserver agreement for overall image quality was good ($\kappa = 0.72$).

Objective image analysis

Overall artefacts

Averaged over all artefacts, mean artefact degree for WFBP was 91.6 ± 81.6 HU. Artefact degree was significantly lower for the iMAR-Algo1 algorithm (58.9 ± 48.5), iMAR-Algo2 algorithm (52.7 ± 46.8 HU) and the iAMRAlgo3 algorithm (51.9 ± 46.1 HU) compared WFBP ($p < 0.004$). There was no significant difference between the three iMAR algorithms ($p > 0.05$) (Table 2).

Mild artefacts

Degree of mild artefacts was similar for WFBP (53.8 ± 24.97 HU) and iMAR-Algo1 (47.9 ± 28.1 HU) ($p = 1$) (Figure 2). We found a significantly lower artefact degree for the iMAR-Algo2 (33.1 ± 12.9 HU) and the iMAR-Algo3 (32.9 ± 11.9 HU) compared with the WFBP and the iMAR-Algo1 ($p < 0.004$ for both).

Severe artefacts

Concerning severe artefacts, all iMAR algorithms reduced artefact degree significantly compared with WFBP (WFBP: 184.4 ± 78.3 HU; iMAR-Algo1: 86.1 ± 36.1 HU; iMAR-Algo2 101.8 ± 43.9 HU; iMAR-Algo3 98.6 ± 44.1 HU; $p < 0.01$, respectively). There was no significant difference between the three different iMAR reconstructions, respectively ($p > 0.02$). The Cardiac

Table 1. Mean scores of subjective image analysis for WFBP and three iMAR algorithms (iMAR-Algo1, iMAR-Algo2 and iMAR-Algo3). Table 1 shows mean values and standard deviation of near and far field scoring for mild and severe artefacts (1: severe artefacts, non-diagnostic; 2: poor image quality, partly non-diagnostic; 3: moderate image quality, limited diagnostic confidence; 4: good image quality, sufficient for diagnosis; 5: excellent image quality, no artefacts)

Artefact degree		WFBP	iMAR-Algo1	iMAR-Algo2	iMAR-Algo3
Overall		3.4 ± 1.3	3.8 ± 0.1	4.3 ± 0.8	4.2 ± 0.7
Mild artefacts	Near field	3.6 ± 0.5	3.8 ± 0.5	4.5 ± 0.5	4.5 ± 0.7
	Far field	4.5 ± 0.6	4.7 ± 0.5	4.9 ± 0.2	4.9 ± 0.3
Severe artefacts	Near field	1.7 ± 0.4	3.8 ± 0.4	3.3 ± 0.5	3.3 ± 0.5
	Far field	2.5 ± 0.6	4.2 ± 0.4	3.5 ± 0.5	3.5 ± 0.5

Table 2. Mean scores of objective image analysis for WFBP and three iMAR algorithms (iMAR-Algo1, iMAR-Algo2 and iMAR-Algo3). Table 2 shows mean values and standard deviation of objective artefact degree for overall artefacts, mild and severe artefacts

	Objective artefact degree (HU)			
	WFBP	iMAR-Algo1	iMAR-Algo2	iMAR-Algo3
Overall	91.6 ± 81.6	58.9 ± 48.5	52.7 ± 46.8	51.9 ± 46.1
Mild artefacts	53.8 ± 24.9	47.9 ± 28.1	33.1 ± 12.9	32.9 ± 11.9
Severe artefacts	184.4 ± 78.3	86.1 ± 36.1	101.8 ± 43.9	98.6 ± 44.1

algorithm showed the strongest artefact reduction compared with the other iMAR algorithms (Figure 3).

DISCUSSION

In this study, we quantitatively and qualitatively assessed the impact of three different iMAR algorithms on artefact burden and image quality in chest CT of patients with thoracic metallic implants. All three iMAR algorithms led to a significant decrease of the artefact degree compared with WFBP. Overall image quality was significantly increased with all iMAR algorithms compared with WFBP. Detailed analysis revealed that the iMAR-Algo2 and the iMAR-Algo3 led to a stronger artefact reduction for mild artefacts than the iMAR-Algo1 and WFBP. However, iMAR-Algo1 enabled the strongest artefact reduction in cases of severe artifacts.

Initial MAR approaches used a one-dimensional linear interpolation to improve CT sinogram data to reduce artefacts. Regarding the high computational time requirements, these methods have not been introduced into clinical routine.[6,16,17] Recently, the combination of linear interpolation and the normalization approach ("normalized metal artefact reduction") have led to a quick and efficient reconstruction performance.[18] The iMAR algorithms used in this study are yet a further improvement to these established algorithms. The mean reconstruction time for one algorithm and the WFBP reconstruction was 4 min and 26 s.

As iMAR algorithms have only recently been introduced, only few studies reported initial results. In accordance with our results for metallic thoracic implants, these studies reported a reduction of metal artefacts from hip prostheses, dental hardware and spine

Figure 2. Chest CT after cardiac surgery and sternotomy reconstructed with WFBP (a), Algo1 (b), Algo2 (c) and Algo3 (d). All reconstructions demonstrate varying degrees of artefacts caused by sternal wires. Postoperative presternal infection was masked by artefacts adjacent to the sternal wires in WFBP and ALGO1 reconstructions. WFBP, weighted filtered back projection.

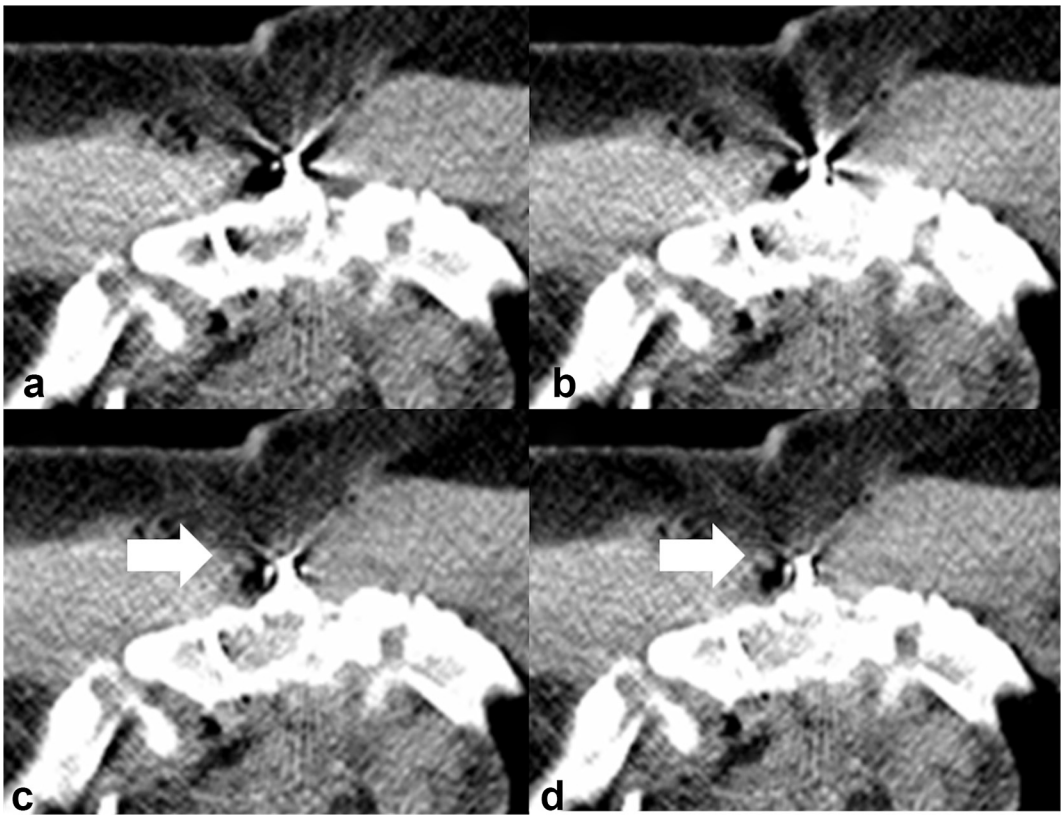

Figure 3. Chest after LVAD implementation reconstructed with WFBP (a), Algo1 (b), Algo2 (c) and Algo3 (d). The WFBP reconstructed image demonstrates severe artefacts produced by LVAD resulting in a non-diagnostic image quality. All iMAR reconstructions lead to a significant artefact reduction and improved image quality. iMAR, iterative metal artefact; LVAD, left ventricular assist device; WFBP, weighted filtered back projection.

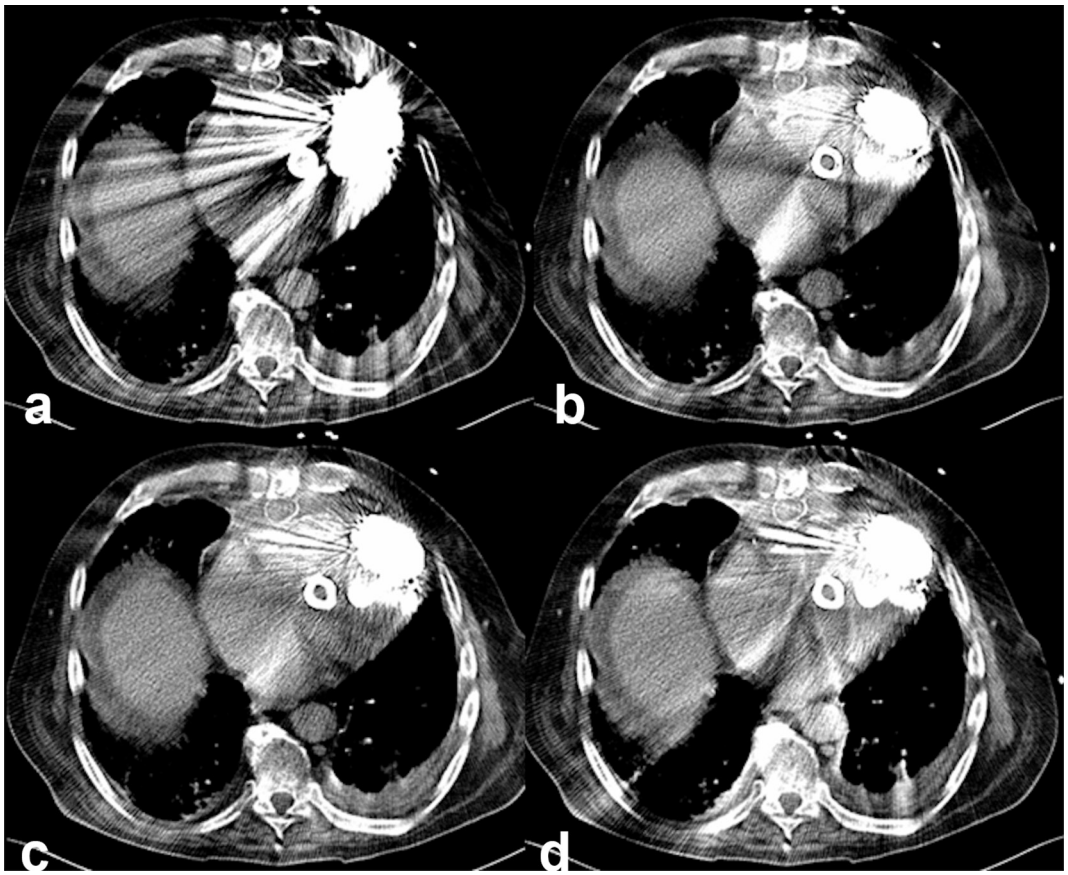

implants when using iterative reconstructions.[9–11] However, in these papers, only a single iMAR algorithm was investigated and compared with filtered back projection.

Although all iMAR algorithms in our study led to a significant reduction of artefact degree compared with WFBP, we also found a significant difference in artefact reduction between the respective iMAR algorithms with iMAR-Algo2 and iMAR-Algo3 being especially helpful in cases with mild artefacts and iMAR-Algo3 in cases with severe artefacts. Although the herein evaluated iterative MAR technique can be employed using conventional single-energy CT acquisition, our results are in accordance with recent studies evaluating iterative MAR algorithms in dual-energy CT with monochromatic reconstructions.[19,20] A significant reduction of artefacts from metallic implants was reported, the degree of which was shown to depend on the implant material and size.[19,21–23] Our results indicate that the effectiveness of the different iMAR algorithms depends on the severity of the artefact and thus on the type and material of the metallic implant. Therefore, iMAR algorithms potentially have to be chosen according to the metallic implant and reconstruction thresholds and other settings of iterative MAR algorithms potentially have to be altered to adjust for different types and locations of metal devices.

A previous study investigated MAR algorithms in chest CT.[24] Huang et al evaluated three different MAR techniques (O-MAR and monochromatic gemstone spectral imaging with and without MAR post processing) and found both MAR post-processing algorithms (O-MAR and MAR post processing for gemstone spectral imaging) to induce new artefacts in chest CT.[24] We did not detect newly induced artefacts for any of the MAR algorithms evaluated in this study. However, both MAR techniques evaluated by Huang et al are from different vendors and, although the specifics remain unknown, are based on different MAR algorithms.

This study has limitations. Our study followed a retrospective study design. Only a small number of patients were included in our study. We did not compare our results to non-iterative MAR algorithms, iMAR algorithms from other vendors or dual-energy CT with monoenergetic reconstructions. Nevertheless, this reflects clinical routine, where only reconstructions from one vendor are available. CT studies from two different CT scanners were included in this study and we did not investigate the differences between the CT scanners. Nevertheless, WFBP and iMAR images were reconstructed for all patients on both scanners. However, we cannot exclude the possibility that results might differ for different CT scanners and scanning parameters.

We investigated three different iMAR algorithms although more algorithms were available. These three iMAR algorithms were preselected as they were specifically designed for thoracic metal implants.

In conclusion, we demonstrated a significant reduction of metal artefacts and a significant increase in overall image quality for three different iMAR algorithms compared with WFBP in chest CT of patients with metallic implants. The iMAR-Algo2 and iMAR-Algo3 were best for mild artefacts while the iMAR-Algo1 was superior for severe artefacts. This indicates that a selection of iMAR algorithms adjusted to patients' metallic implants and artefact severity can help to improve image quality in chest CT.

REFERENCES

1. Konen E, Yellin A, Greenberg I, Paley M, Shulimzon T, Wolf M, et al. Complications of tracheal and thoracic surgery: the role of multisection helical CT and computerized reformations. *Clin Radiol* 2003; **58**: 341–50. doi: https://doi.org/10.1016/S0009-9260(03)00057-6
2. Casha AR, Manché A, Gatt R, Duca E, Gauci M, Schembri-Wismayer P, et al. Mechanism of sternotomy dehiscence. *Interact Cardiovasc Thorac Surg* 2014; **19**: 617–21. doi: https://doi.org/10.1093/icvts/ivu184
3. Alhalawani AM, Towler MR. A review of sternal closure techniques. *J Biomater Appl* 2013; **28**: 483–97. doi: https://doi.org/10.1177/0885328213495426
4. Secchi F, De Cecco CN, Spearman JV, Silverman JR, Ebersberger U, Sardanelli F, et al. Monoenergetic extrapolation of cardiac dual energy CT for artifact reduction. *Acta Radiol* 2015; **56**: 413–8. doi: https://doi.org/10.1177/0284185114527867
5. Habets J, Symersky P, Leiner T, de Mol BA, Mali WP, Budde RP. Artifact reduction strategies for prosthetic heart valve CT imaging. *Int J Cardiovasc Imaging* 2012; **28**: 2099–108. doi: https://doi.org/10.1007/s10554-012-0041-5
6. Kalender WA, Hebel R, Ebersberger J. Reduction of CT artifacts caused by metallic implants. *Radiology* 1987; **164**: 576–7. doi: https://doi.org/10.1148/radiology.164.2.3602406
7. Filograna L, Magarelli N, Leone A, Guggenberger R, Winklhofer S, Thali MJ, et al. Value of monoenergetic dual-energy CT (DECT) for artefact reduction from metallic orthopedic implants in post-mortem studies. *Skeletal Radiol* 2015; **44**: 1287–94. doi: https://doi.org/10.1007/s00256-015-2155-z
8. Stolzmann P, Winklhofer S, Schwendener N, Alkadhi H, Thali MJ, Ruder TD. Monoenergetic computed tomography reconstructions reduce beam hardening artifacts from dental restorations. *Forensic Sci Med Pathol* 2013; **9**: 327–32. doi: https://doi.org/10.1007/s12024-013-9420-z
9. Subhas N, Primak AN, Obuchowski NA, Gupta A, Polster JM, Krauss A, et al. Iterative metal artifact reduction: evaluation and optimization of technique. *Skeletal Radiol* 2014; **43**: 1729–35. doi: https://doi.org/10.1007/s00256-014-1987-2
10. Wuest W, May MS, Brand M, Bayerl N, Krauss A, Uder M, et al. Improved image quality in head and neck CT using a 3D iterative approach to reduce metal artifact. *AJNR Am J Neuroradiol* 2015; **36**: 1988–93. doi: https://doi.org/10.3174/ajnr.A4386
11. Kotsenas AL, Michalak GJ, DeLone DR, Diehn FE, Grant K, Halaweish AF, et al. CT metal artifact reduction in the spine: can an Iterative reconstruction technique improve visualization? *AJNR Am J Neuroradiol* 2015; **36**: 2184–90. doi: https://doi.org/10.3174/ajnr.A4416
12. Lell MM, Meyer E, Schmid M, Raupach R, May MS, Uder M, et al. Frequency split metal artefact reduction in pelvic computed tomography. *Eur Radiol* 2013; **23**: 2137–45. doi: https://doi.org/10.1007/s00330-013-2809-y
13. Boos J, Sawicki LM, Lanzman RS, Thomas C, Aissa J, Schleich C, et al. Metal artifact reduction (MAR) based on two-compartment physical modeling: evaluation in patients with hip implants. *Acta Radiol* 2017; **58**. doi: https://doi.org/10.1177/0284185116633911
14. Sonoda A, Nitta N, Ushio N, Nagatani Y, Okumura N, Otani H, et al. Evaluation of the quality of CT images acquired with the single energy metal artifact reduction (SEMAR) algorithm in patients with hip and dental prostheses and aneurysm embolization coils. *Jpn J Radiol* 2015; **33**: 710–6. doi: https://doi.org/10.1007/s11604-015-0478-2
15. Landis JR, Koch GG. The measurement of observer agreement for categorical data. *Biometrics* 1977; **33**: 159–74. doi: https://doi.org/10.2307/2529310
16. Mahnken AH, Raupach R, Wildberger JE, Jung B, Heussen N, Flohr TG, et al. A new algorithm for metal artifact reduction in computed tomography: in vitro and in vivo evaluation after total hip replacement. *Invest Radiol* 2003; **38**: 769–75. doi: https://doi.org/10.1097/01.rli.0000086495.96457.54
17. Beister M, Kolditz D, Kalender WA. Iterative reconstruction methods in X-ray CT. *Phys Med* 2012; **28**: 94–108. doi: https://doi.org/10.1016/j.ejmp.2012.01.003
18. Meyer E, Raupach R, Lell M, Schmidt B, Kachelriess M. Normalized metal artifact reduction (NMAR) in computed tomography. *Med Phys* 2010; **37**: 5482–93. doi: https://doi.org/10.1118/1.3484090
19. Lee YH, Park KK, Song HT, Kim S, Suh JS. Metal artefact reduction in gemstone spectral imaging dual-energy CT with and without metal artefact reduction software. *Eur Radiol* 2012; **22**: 1331–40. doi: https://doi.org/10.1007/s00330-011-2370-5
20. Morsbach F, Wurnig M, Kunz DM, Krauss A, Schmidt B, Kollias SS, et al. Metal artefact reduction from dental hardware in carotid CT angiography using iterative reconstructions. *Eur Radiol* 2013; **23**: 2687–94. doi: https://doi.org/10.1007/s00330-013-2885-z
21. Meinel FG, Bischoff B, Zhang Q, Bamberg F, Reiser MF, Johnson TR. Metal artifact reduction by dual-energy computed tomography using energetic extrapolation: a systematically optimized protocol. *Invest Radiol* 2012; **47**: 406–14. doi: https://doi.org/10.1097/RLI.0b013e31824c86a3
22. Guggenberger R, Winklhofer S, Osterhoff G, Wanner GA, Fortunati M, Andreisek G, et al. Metallic artefact reduction with monoenergetic dual-energy CT: systematic ex vivo evaluation of posterior spinal fusion implants from various vendors and different spine levels. *Eur Radiol* 2012; **22**: 2357–64. doi: https://doi.org/10.1007/s00330-012-2501-7
23. Wang Y, Qian B, Li B, Qin G, Zhou Z, Qiu Y, et al. Metal artifacts reduction using monochromatic images from spectral CT: evaluation of pedicle screws in patients with

scoliosis. *Eur J Radiol* 2013; **82**: e360–e366. doi: https://doi.org/10.1016/j.ejrad.2013.02.024

24. Huang JY, Kerns JR, Nute JL, Liu X, Balter PA, Stingo FC, et al. An evaluation of three commercially available metal artifact reduction methods for CT imaging. *Phys Med Biol* 2015; **60**: 1047–67. doi: https://doi.org/10.1088/0031-9155/60/3/1047